Heliyon 10 (2024) e40495

Contents lists available at ScienceDirect

Heliyon

journal homepage: www.cell.com/heliyon

Research article

Nano-pumice derived from pumice mine waste as a low-cost electrode catalyst for microbial fuel cell treating edible vegetable oil refinery wastewater for bioenergy generation and reuse

Fatemeh Eslami [a,b], Kamyar Yaghmaeian [c,d], Reza Shokoohi [e], Roohallah Sajjadipoya [f], Alireza Rahmani [e], Hedieh Askarpur [g,h], Abbas Norouzian Baghani [i], Hossein Jafari Mansoorian [e,*], Farshid jaberi Ansari [j]

[a] Department of Environmental Health Engineering, School of Health, Jiroft University of Medical Sciences, Jiroft, Iran
[b] Department of Environmental Health Engineering, School of Public Health, Iran University of Medical Sciences, Tehran, Iran
[c] Department of Environmental Health Engineering, Tehran University of Medical Sciences, Tehran, Iran
[d] Center for Solid Waste Research, Institute for Environmental Research, Tehran University of Medical Sciences, Tehran, Iran
[e] Department of Environmental Health Engineering, Faculty of Health and Research Center for Health Sciences, Hamadan University of Medical Sciences, Hamadan, Iran
[f] Department of Environmental Health Engineering, Jondishapoor University of Medical Sciences, Ahwaz, Iran
[g] Jiroft University of Medical Sciences, Jiroft, Iran
[h] Clinical Research Development Unit, Imam Khomeini Hospital, Jiroft University of Medical Sciences, Jiroft, Iran
[i] Environmental Health Research Center, Lorestan University of Medical Sciences, Khorramabad, Iran
[j] Department of Medical Nanotechnology, School of Advanced Technologies in Medicine, Tehran University of Medical Sciences, Tehran, Iran

ARTICLE INFO

Keywords:
Pumice mine waste
Microbial fuel cell
Electrode surface area
Anode catalyst
Industrial wastewater

ABSTRACT

This study aimed to assess nano-pumice (NP) from pumice mining waste as a local, cost-effective anode catalyst in microbial fuel cells (MFCs) for treating edible vegetable oil refinery wastewater (EVORW) and generating bioenergy. Pumice mining waste was converted into nano in three stages: crushing up to ≤3 cm, reducing the size of the previous step particles to 150 μm and converting the previous step particles to <100 nm. Nano-pumice prepared was coated on the carbon cloth (CC) to increase anode surface area of MFC. Two MFCs were utilized, with MFC-1 serving as a control and MFC-2 incorporating a CC electrode coated with nano-pumice. The surface morphology, elemental and chemical composition, and textural characterization of CC, pumice, NP, and CC coated with NP were analyzed using FE-SEM, EDX, XRF, and BET techniques. MFC-2 achieved a maximum power density of 30±4W/m^3 at a current density of 55±5A/m^3. The MFC-1 reached a maximum power density of 18±4W/m^3 at a current density of 35±6A/m^3. In MFC-2, the EVORW treatment achieved maximum removals of COD (94 ± 2 %), NH_4^+-N (85 ± 4 %), TP (76 ± 5 %), SO_4^{2-} (68 ± 6 %), TSS (81 ± 2 %), and TDS (73 ± 1 %). MFC-1 achieved removal efficiencies of 66 ± 3 % for COD, 57 ± 6 % for NH_4^+-N, 48 ± 3 % for TP, 45 ± 3 % for SO_4^{2-}, 65 ± 3 % for TSS, and 61 ± 1 % for TDS. MFC-2 power density rose significantly, reaching 61 ± 3 % (1.6 times) higher than MFC-1and it also demonstrated a superior ability to improve raw wastewater quality compared to MFC-1. The MFC with the CC/NP anode exhibited both excellent power production and high COD removal efficiency, making nano-pumice a suitable anode catalyst for MFC applications.

* Corresponding author.
E-mail address: h.mansoorian@yahoo.com (H. Jafari Mansoorian).

https://doi.org/10.1016/j.heliyon.2024.e40495
Received 29 July 2024; Received in revised form 26 October 2024; Accepted 15 November 2024
Available online 19 November 2024

1. Introduction

The vegetable oil production industry in Iran is undergoing a period of accelerated growth driven by rising demand for edible oil, a phenomenon which can be attributed to population growth and increased food consumption in emerging nations [1]. The progressive enhancement of living standards and alterations to dietary habits have resulted in a gradual surge in the demand for edible oils. Iran currently has 42 facilities engaged in the production of vegetable oils, with an annual production capacity of approximately 2 million tons [2]. Plant oils are of great importance to global nutrition, and are used extensively in food preservation and preparation [3]. According to the Food and Agriculture Organization (FAO) of the United Nations, the annual consumption of vegetable oil for food purposes is anticipated to reach 210 million tons by 2024 [4]. A substantial impediment to the advancement of this industry is the environmental hazard posed by the release of contaminants, such as polluted wastewater, which threaten the environment, groundwater, surface water, and public health and safety [5].

The release of wastewater from vegetable oil producing refineries into natural water sources has been identified as a significant source of pollution. This wastewater is characterized by high levels of organic load (i.e., COD and BOD), as well as large volumes of oil and fat, suspended particles, and turbidity. The resulting pollution renders these water sources unfit for use [6]. Moreover, the introduction of this wastewater into the sewage collection network and subsequently into the municipal wastewater treatment plant gives rise to a number of issues, including network obstructions, disruptions in the settling units, a notable reduction in the concentrations of dissolved oxygen levels in the aeration tanks, disruptions in the activity of microorganisms, and overall faults in the operation of the treatment system [7]. Furthermore, the discharge of this wastewater into surface water results in the uncontrolled growth of algae, the creation of suspended compounds and layers associated with oil, and a change in the color of the surrounding water. Therefore, it is imperative to carry out appropriate treatment of such effluent in accordance with environmental regulations and standards before releasing it into the environment [8].

A variety of technologies have been employed in the treatment of wastewater from edible vegetable oil production refineries, including physicochemical methods (such as coagulation/flocculation and adsorption), membrane processes, advanced oxidation processes, electrochemical methods (such as electrocoagulation), and biological treatment methods [9–13]. Nevertheless, these techniques necessitate a considerable input of energy and incur significant operational costs. Moreover, the current wastewater treatment technologies are insufficiently sustainable to meet the ever-increasing demand for water sanitation. Therefore, it is imperative that edible vegetable oil production facilities implement an appropriate wastewater treatment system in order to facilitate the reuse of wastewater as an alternative water supply and the generation of valuable products such as bioenergy [12,14]. Bioelectrochemical systems (BESs) represent a technique that has been extensively investigated for its potential applications in wastewater treatment and energy generation. This method effectively mitigates pollutants without the necessity of adding chemical components [15].

The bioelectrochemical system (BES) is a device that uses microbes as catalysts to drive oxidation and/or reduction reactions at electrodes, thereby extracting energy from organic matter present in wastewater or organic waste. In these devices, microbial communities must utilize either a solid electron acceptor (bioanode) or an electron donor (biocathode) as a crucial component of their metabolic processes. The potential applications for this technology are numerous and include wastewater treatment, power production, bioremediation, and the production of valuable chemicals. Consequently, BESs are recognized as an environmentally friendly technology for wastewater treatment [16,17]. BES can be classified as environmentally friendly technologies because they facilitate the conversion of organic substances and waste into energy or chemicals in a manner that does not harm the environment. Microbial fuel cells (MFCs) represent a significant category of BES, comprising over 80 % of such systems.

MFCs demonstrate the potential to convert the chemical energy stored in organic chemicals and biodegradable materials into electrical energy through the use of microorganisms, while also effectively treating wastewater [18,19]. Although MFCs have practical applications, their acceptance for field applications has been limited due to the costly materials used in the fabrication of MFCs or synthesis of electrode catalysts and low power density. Additionally, the properties of the anode material greatly influence the power generation of MFCs, as the anode is the primary site for exoelectrogen attachment and electron transfer. Therefore, a high-performance anode composite/structure is essential to improve the power outputs of MFCs [20].

Various nanostructured materials such as polyaniline-polypyrrole composite hydrogel [21], polypyrrole/chitosan [22], TiO_2 nanotube arrays (TNA) [23], Heteroatom-doped porous carbon nanoparticle-decorated carbon cloth (HPCN/CC) [24], iron oxide (Fe_2O_3)-MXene (Ti_3C_2) [17], molybdenum oxides (MoO_x) are doped with various types of non-metal atoms (N, P, and S) [25], $CoFe_2O_4$ nanoparticles [19], Co_8FeS_8-$FeCo_2O_4$/N-CNTs@CF [26], nano-molybdenum disulfide/carbon nanotubes [27], Polyaniline-MXene [28], MnO_2@MXene [20], Ti_3C_2 MXene with NH_4^+ [29], Nickel-Cobalt oxides coated on polypyrrole nanotubes [30], nano hydroxyapatite (nHA)/CNTs [31], and FeS_2@CNT [32] had been used to modify the MFC electrodes and fabricate high-performance MFC anodes to increase the MFC power density output. However, the high cost of these materials and the complex synthesis methods involved have so far hindered their profound application in the system [33,34]. Therefore, in order to reduce the cost of the MFC and to make it a commercially viable proposition, it is necessary to devote greater attention to the development of low-cost catalysts with high performance characteristics. In other words, the selection of potential anode materials and anode surface modification, as well as the analysis of the impact of surface characteristics on microbial energy production, are crucial for enhancing the power generation capacity of MFCs [32,35].

Therefore, a substantial number of investigations are necessary to identify cost-effective materials that can reduce the production costs of these systems and enhance their efficiency in terms of bioenergy generation and wastewater treatment. This study examined the potential of utilizing natural geomaterials or locally sourced minerals, in conjunction with nanomaterials derived from pumice

mine waste, as catalysts for anode electrodes. Pumice is a lightweight volcanic rock that occurs in a variety of colors and contains high amounts of silicon and aluminum. It is a naturally occurring pozzolan, formed when lava cools and solidifies. This compound is extensively distributed in several areas of Iran, including Kurdistan, Ardabil, Tabriz, Kermanshah, Alborz, Kerman, Sistan and Baluchestan, and Khorasan. It is widely and easily obtainable at a modest price [36,37]. Pumice exhibits high chemical stability, high mechanical strength, high porosity, and high specific surface area. These qualities and benefits have led to its utilization as an absorbent to eliminate a range of contaminants from water environments [38]. Nevertheless, the use of this catalyst at nano-scales for anodic purposes in MFC has yet to be investigated.

The efficacy of MFCs in the removal of contaminants from a range of wastewater sources, including industrial, domestic, food processing, and animal waste, has been demonstrated through research. The potential for the generation of sustainable energy through the treatment and reuse of wastewater has attracted global attention [31,39]. The edible vegetable oil refinery's wastewater (EVORW) contains a significant amount of organic matter that can be employed for the generation of bioelectricity through the use of microbial fuel cells (MFC). In this study, MFCs were created using both nano-pumice, a low-cost catalyst derived from local pumice mine waste, and without it. The goal was to compare the voltage and power generation of two types of MFCs, as well as their effectiveness in removing organic matter and nutrients from edible vegetable oil wastewater for potential reuse.

2. Material and methods

2.1. Electrode preparation

The anode and cathode electrodes were constructed using carbon cloth. Prior to use, the cloth was soaked in a wetting agent for 24 h to remove surface impurities, then rinsed with deionized water and air-dried for another 24 h. The pumice used as an electrode catalyst in this study was sourced from mining waste in the Qorveh region of Kurdistan province, Iran. At first, the necessary quantity of pumice grains underwent numerous washes with distilled water to eliminate any contaminants. Then, the cleaned granules were subjected to a drying process at 103°C for 6 h using a forced air-drying device to remove any moisture present. During the subsequent phase, the pumice grains were pulverized using a cone crusher until they reached dimensions that were either smaller or equal to 3 cm. The particle size was further reduced to 150 μm using a micronizer. The resulting particles were mixed with water and fed into the satellite mill chamber to achieve dimensions below 100 nm. The milled particles were then directed to a spray dryer. At this point,

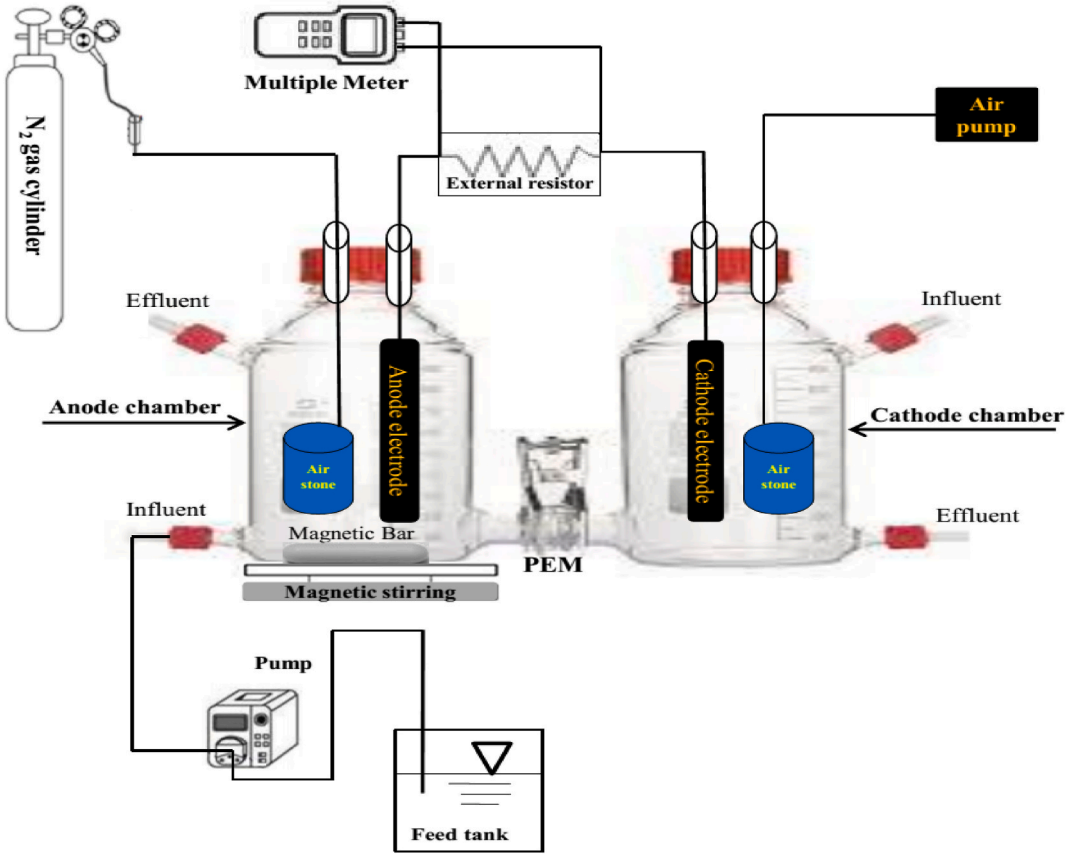

Fig. 1. Microbial fuel cell experimental setup.

centrifugation was employed to separate the bigger particles from the tiny particles in the mixture. The nanoparticles section was dried using a spray dryer to remove water molecules from the pores on the particle surfaces. Once dry, the nano-pumice particles were immediately ready for use. A pressure rolling technique, as outlined in previous studies, was employed to apply a layer of nano-pumice onto carbon cloth [40–42]. Then, ethanol was combined with nano-pumice and the combination was meticulously mixed with a PTFE binder using ultrasonic mixing in order to create a catalytic paste. During the next phase, the mixture was used for both the anode and one surface of the cathode using a rolling machine. During the last phase, the electrodes that had been manufactured were subjected to heat treatment at a temperature of 160^{o}C in an oven in order to dry them before usage. Finally, the electrodes were divided into squares of 2 $\times$ 2 cm for practical purposes.

2.2. Real edible vegetable oil refinery wastewater (EVORW)

Wastewater samples were collected from a nearby edible vegetable oil refinery in Tehran, Iran. Sampling was performed once every three days. A total of 48 samples were taken from after passing through a grease and oil trap and before treatment in order to obtain a clear picture of the quality of effluent. It was then stored in PVC bottles at a pH 4 and a temperature below 4 °C to prevent biodegradation of the wastewater. The physicochemical properties of the samples such as pH, temperature, electric conductivity (EC), total solids (TS), total suspended solids (TSS), total dissolved solids (TDS), turbidity, chemical oxygen demand (COD), biochemical oxygen demand (BOD), ammonia nitrogen (NH_4^+-N), and total phosphorus (TP), were analyzed using standard methods [43]. The pH, temperature and electric conductivity parameters were examined in situ. The various concentrations of wastewater were created by diluting with distilled water.

2.3. MFC construction and operation

In this study, two MFCs, designated MFC-1 and MFC-2, were constructed. MFC-1 was employed as the control, with no modifications made to the electrode. In contrast, MFC-2 was constructed with a catalyst-modified electrode. Both MFCs were made using 500 mL glass bottles and designed as dual-chamber systems. A proton exchange membrane (PEM) comprising Nafion (NAFION 117, Sigma-Aldrich) separates the chambers. Prior to use, the PEM was cleaned in accordance with the methodology outlined in a previous study [44]. The anode electrode was composed of carbon cloth coated with nano-pumice, which served as the catalyst. These electrodes were connected by copper wire, which was linked to an external resistor. A digital multimeter was connected to the resistor in order to measure the output voltage generated by the MFC. Fig. 1 depicts the schematic view of the MEC used in the study. The polarization curve was obtained by measuring the output voltage as a function of external resistance, with values ranging from 1000 to 25 Ω. Once the maximum stable voltage was reached, the most suitable resistance was introduced into the circuit.

The MFCs were operated in batch mode. The whole operation time of the MFCs reactor was 120 days. During the start-up phase, the MFCs were run at open-circuit voltage (OCV) conditions, as previously described. The anode chamber was inoculated with sodium acetate, anaerobic digester sludge that had undergone thermal pre-treatment, phosphate buffer, minerals, and vitamins [44]. Subsequently, the process was conducted with actual wastewater as the anolyte. 2-bromoethanesulfonate was introduced to the sample in order to suppress the activity of methanogenic bacteria. To eliminate oxygen and establish anaerobic conditions in the anode chamber, nitrogen gas was introduced into the chamber for a period of 20 min at the outset of the procedure. The cathode chamber was filled with phosphate buffer, specifically a solution containing 50 mM of potassium dihydrogen phosphate, which served as the catholyte. The dissolved oxygen concentration was maintained at a level between 4 and 5 mg/L by means of continuous aeration, which was achieved through the use of an aquarium air pump. Once the system had reached a consistent voltage output during the acclimation phase, it proceeded to the experimental phase, utilizing actual wastewater from the edible vegetable oil refining factory. The contents of the anode chamber were vigorously stirred using a magnetic stir bar. The system was operated at a temperature of 35 $\pm$ 2 °C and at a neutral pH (between 6.8 and 7.2). A phosphate buffer solution was employed to adjust the pH. Subsequently, when the voltage generated fell below 100 mV, the analyte was replaced. An external mediator was not utilized within the anode chamber. Furthermore, because the wastewater utilized as fuel in the system had a high electrical conductivity, there was no need to include an electrolyte in the system.

2.4. Analysis and calculation

The surface morphology, elemental and chemical composition and textural characterization of carbon cloth (CC), pumice (P), nano-pumice (NP), and carbon cloth coated with nano-pumice were conducted using field emission scanning electron microscopy (FE-SEM, S4160 manufactured by HITACHI Co., Japan), energy dispersive X-ray spectrum (EDX) using the same instrument, X-ray fluorescence analysis(XRF, Xpert Philips PW 3040/60, Lum Cu, The Netherlands), and Brunauer–Emmett–Teller (BET, Belsorp mini II, Bel model, Japan) techniques. In order to ascertain the efficacy of the bio-treatment process employed by the MFC for the purpose of reuse, a series of physicochemical analyses were conducted on wastewater samples, with a view to determining the levels of COD, BOD_5, NH_4^+-N, P, SO_4^{2-}, TSS and TDS present. These analyses were carried out in accordance with the relevant standard methods. In addition, a digital multi-meter was used to measure the voltage and current generated by the system, with a view to assessing its bioenergy production capacity.

The current was determined by formula I = U/R, where R represents the resistance (Ω) and U (V) represents the voltage across the resistor. The power was determined using equation P = I $\times$ V, where P (W) and I (A) represents power and current. The power density and current density were determined by dividing the current and power by the reactor's volume, respectively. The formulas used were

$CD\ (A/m^3) = I/$reactor volume and $PD\ (W/m^3) = P/$reactor volume. The coulombic efficiency (CE) and energy efficiency (EE) were calculated using the specified formulas, as previously outlined [45]:

$$CE = M \int_0^t Idt \Big/ FnV\Delta COD \quad 1)$$

$$EE = \int_0^t PIdt \Big/ \Delta Hn_s \quad 2)$$

where M is the molecular weight of oxygen (O_2), I is current generated during whole batch cycle (A), t (d) is the running time of MFC reactor, F is Faraday's constant (96485C/mol-electrons), V is anolyte volume (L), Δ H(J/mol) is the heat of combustion and n_s is the amount (mol) of substrate provided.

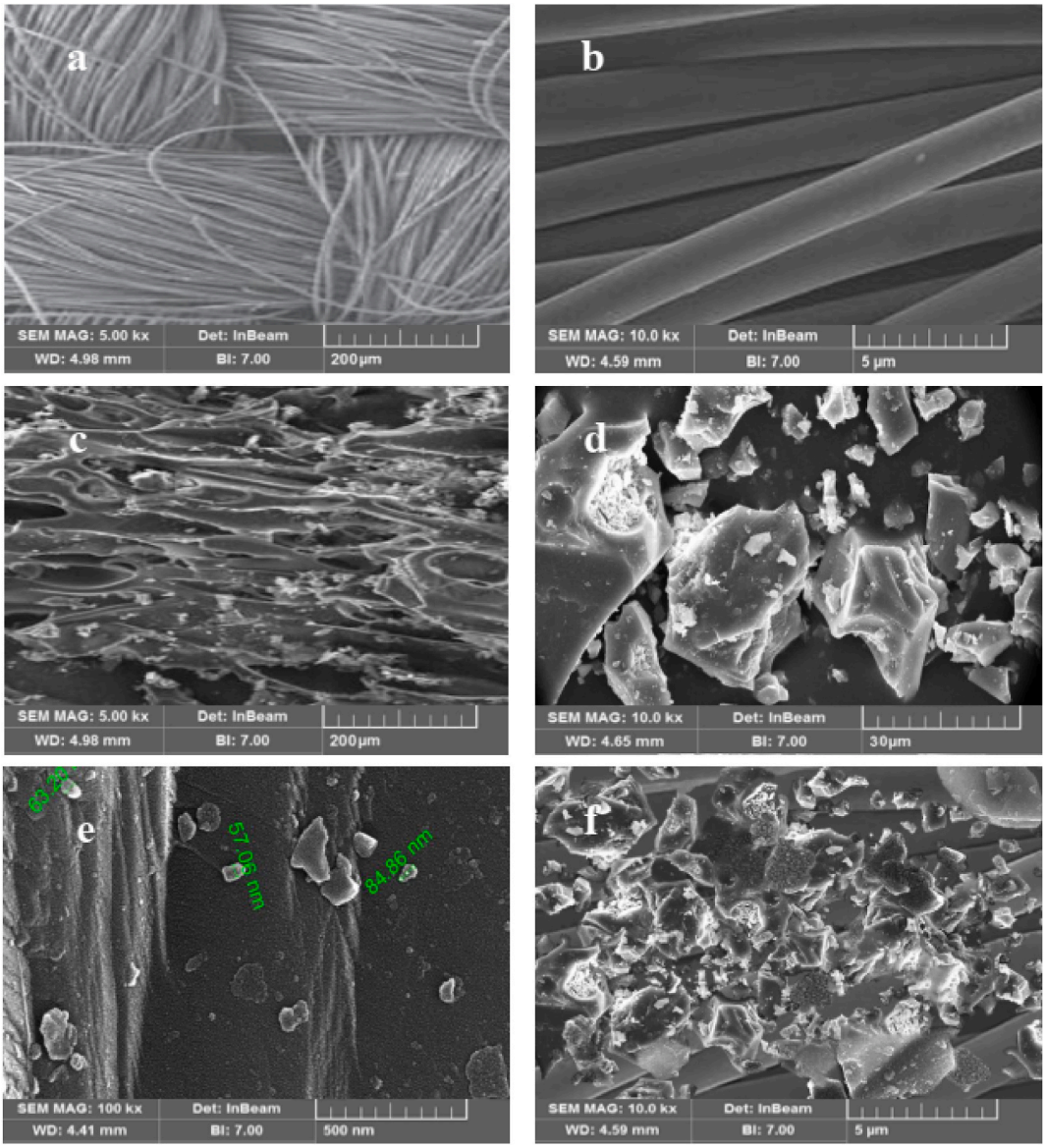

Fig. 2. FE-SEM images of (a and b) the Bare Carbon cloth (c) Pure pumice (d and f) nano-pumice (e) CC/NP.

3. Results and discussion

3.1. Morphological, elemental, chemical and textural characterization of samples

The surface morphologies of the pure carbon cloth (CC), pumice, nano-pumice (NP), and CC/NP were observed using FE-SEM and are displayed in Fig. 2. As illustrated in Fig. 2a and b, prior to the coating procedure, the fiber surface of CC is characterized by a smooth texture. Liu et al. and Cho et al. have pointed to the smooth surface of the carbon cloth fiber before the coating process [46,47]. The surface morphology of the pumice, as depicted in Fig. 2c, displays notable porosity, an uneven texture, and a somewhat rough surface. The result well corresponded with the previous studies that the pumice had high porosity, irregular shapes and relatively rough surfaces [38,48].

As illustrated in Fig. 2d and e, the nano-pumice micrograph reveals particles with an average size of less than 100 nm, which indicates that the nano-pumice manufacturing process was effective. The FE-SEM study results demonstrate that this structure enhances the sorption capacity of pollutants by producing porosity and increasing the number of channels. Eslami et al. (2020) also reported nano-pumice has a porous surface with dimensions in the range of <100 nm [49]. Upon coating the carbon cloth with nano-pumice, a uniform distribution of solid particles was observed across the surface of the cloth, exhibiting a random pattern. After the coating procedure, the surface of the CC became rough and adorned with nano-pumice particles (Fig. 2f), indicating the presence and arrangement of these particles on the fiber of the CC.

The XRF and EDX analysis revealed the chemical and elemental composition of the pumice, which is presented in Table 1. The XRF revealed that the primary components of pure pumice are SiO_2, Al_2O_3, K_2O, Fe_2O_3, and Na_2O, with SiO_2 being the most abundant. Additional constituents, including CaO, MgO, MnO, ZrO_2, and P_2O_5 were also identified in their composition. Other studies have referred to SiO_2 as the main composition of the pumice structure [49,50]. The EDX analysis revealed the existence of silicon (Si) and aluminum (Al) as the primary components in the oxide, along with oxygen. Furthermore, trace elements, including carbon (C), sodium (Na), magnesium (Mg), potassium (K), calcium (Ca), iron (Fe), and zirconium (Zr) were identified. The inclusion of silicon, aluminum, and iron oxides in pumice materials indicates the robustness and durability of pumice. Similar results have been reported by Dagwa et al. and Khataee et al. [37,51].

The study investigated the alterations in the specific surface area and pore volume as a result of coating nano-pumice particles on CC by N_2 adsorption experimentation. Table 2 shows that the CC/nano-pumice composite had more surface area and pore volume compared to the pure pumice and CC samples, respectively. The variations observed can be ascribed to the existence of nanoscale pumice particles on the CC samples. Khataee et al. (2018) reported the surface area and pore volume of the ZrO_2-pumice and ZrO_2-tuff nanocomposites were higher than those of the pure pumice and tuff samples, respectively. These differences were attributed to the presence of nanosized ZrO_2 particles on the pumice and tuff [37]. It was speculated that the nano-pumice particles primarily adhered to the surface of the CC. Additionally, CC/NP offered a conducive and biocompatible extensive surface area for the growth of bacteria, a desirable characteristic for an anode to enhance the efficiency of MFC. The results of the present study are comparatively better than Eslami et al. (2018) that reported specific surface area and pore volume 6.4693 m^2/g and 4.3 cm^3/g for nano-pumice, and 9.79 m^2/g and 4.79 cm^3/g for pumice/HDTM.Br nano composite, respectively [49]. Also, the results of the present study are comparable to Khataee et al. (2018) research where a surface area 1.02, 0.92, 5.87, 1.16 m^2/g and pore volume 0.23, 0.21, 1.35 and 0.27 cm^3/g for pure pumice, tuff, ZrO_2-pumice and ZrO_2-tuff nanocomposites has been reported, respectively [37].

3.2. Edible vegetable oil refinery wastewater characterization

Analysis of wastewater samples is essential to understand changes in pollution levels over time, to determine the composition and concentration of various substances, and to effectively manage the treatment process. Treatment efficiency is greatly influenced by the presence of chemical and organic pollutants. Wastewater from edible oil manufacturers contains a significant amount of both organic and inorganic substances. Table 3 provides a summary of the attributes of the wastewater samples. As can be seen in Table 3, the effluent from the edible vegetable oil refinery had elevated levels of COD and BOD_5 concentrations. The values of COD and BOD_5 ranged from 23768 ± 2690 mg/L to 9745 ± 2070 mg/L, respectively. The BOD_5/COD ratio, also known as the biodegradability factor, is a measure of the ability of the organic matter in wastewater samples to be degraded by biological processes. A high ratio suggests that biological treatment methods can be used in this particular case. The bio-degradability index (BI) is defined as the ratio of BOD_5 to COD. The metric BI quantifies the viability of using edible vegetable oil refinery wastewater for additional biological treatment. Prior to selecting a bio-based wastewater treatment, it is crucial to be aware of the biodegradability index (BI) of the untreated wastewater. If the BOD/COD ratio is greater than 0.6, then the waste can be considered highly biodegradable. Seeding is necessary for biological treatment of wastewater with a BOD/COD ratio of 0.3–0.6, although this approach may result in a delayed treatment process. If the ratio of BOD/COD is less than 0.3, biodegradation does not occur, and therefore, biological treatment is not possible [9]. The study

Table 1
The chemical and elemental composition from the XRF and EDX analysis of pumice.

	Type of analysis	Al_2O_3	CaO	Fe_2O_3	K_2O	MgO	MnO	Na_2O	P_2O_5	SiO_2	ZrO_2
Pumice	**XRF (%)**	8.275	0.782	1.591	4.312	0.438	0.253	1.207	0.044	48.069	0.052
		C	**O**	**Si**	**Al**	**K**	**Na**	**Ca**	**Fe**	**Mg**	**Zr**
	EDX (%)	0.33	64.58	24.22	5.94	1.74	0.62	0.95	1.03	0.59	0.00

Table 2
Textural characteristics of the samples.

Sample	specific surface area (m^2/g)	Pore volume (cm^3/g)
Bare Carbon cloth	28.15	0.082
Pure pumice	1.24	0.33
nano-pumice	7.11	5.12
CC/nan-opumice (nano-pumice coated on carbon cloth)	63.48	0.117

Table 3
Physicochemical characterization of the edible vegetable oil refinery wastewater.

Parameter	Unit	Value
COD	mg/L	23768 ± 2690
BOD_5	mg/L	9745 ± 2070
Total Phosphorus	mg/L	125 ± 8
ammonia Nitrogen	mg/L	293 ± 14
TS	mg/L	6830 ± 1024
TSS	mg/L	2315 ± 285
TDS	mg/L	4694 ± 387
SO_4^{2-}	mg/L	853 ± 104
Oil & Grease	mg/L	4721 ± 595
pH	–	9.21 ± 0.74
Turbidity	NTU	2070 ± 315
electrical conductivity	μs/cm	5910 ± 927
BI (BOD/COD ratio)	–	0.4 ± 0.03
Temperature	°C	44 ± 5

found that the Biological Index (BI) of the effluent from the edible vegetable oil refinery was 0.4 ± 0.03.

The concentration of total suspended solids (TSS) and turbidity in the wastewater samples extracted directly from the effluent drain of the vegetable oil refinery was high, with values ranging from 2315 ± 285 mg/L and 2070 ± 315NTU. This is because the samples were not subjected to any sedimentation processes. The presence of suspended solids in the effluent indicates that they contribute to the levels of BOD_5 and COD in the wastewater. The BOD_5, COD, and TSS values indicate that the process wastewater has a fluctuating high contamination level. The study investigated ammonia nitrogen (NH_4^+-N) and found high levels of NH_4^+-N, ranging from 293 ± 14 mg/L. This suggests that the most of the nitrogen is present in the form of ammonia, which is commonly found in wastewater refineries that process edible vegetable oil. The EVORW samples had an alkaline pH, ranging from 9.21 ± 0.74, indicating a significant level of alkalinity. The neutralization process in soap production introduces phosphorus (P) content into wastewater through the sodium salts of the fatty acids soap stock. Vegetable oil effluent contains significant levels of phosphorus due to the extensive use of phosphoric acid during in the degumming process. Similarly, EVORW is characterized by a significant presence of chemical contaminants, including oil

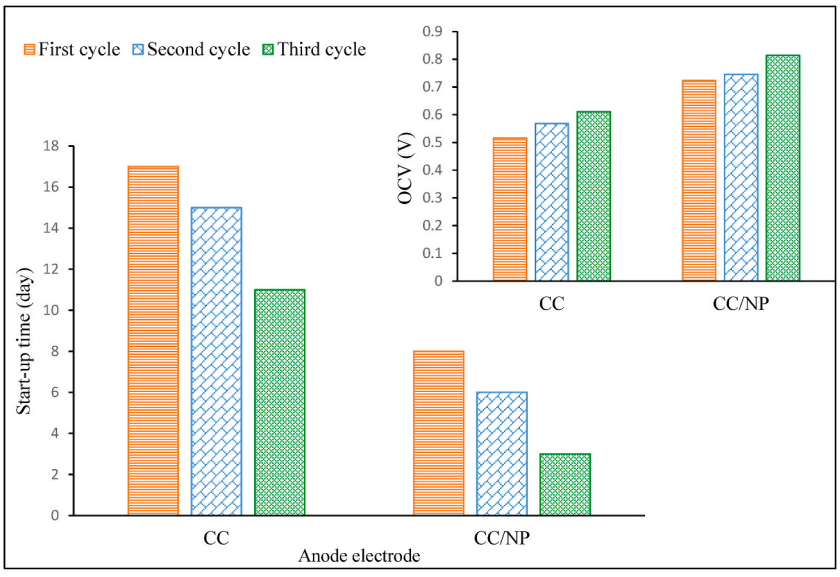

Fig. 3. Start-up times and OCV of different anodes.

and grease (4721 ± 595 mg/L) and sulfate (SO_4^{2-}, 853 ± 104 mg/L).

3.3. MFC performance during the start-up and acclimation phase

The growth of a biofilm of electroactive bacteria on the anode electrodes is a critical feature in maintaining organic matter and facilitating power generation in microbial fuel cells (MFCs). Fig. 3 shows the performance of MFC-1 and MFC-2 at start-up and in open circuit voltage (OCV) mode. As shown in Fig. 3, during the acclimatization phase, MFC-1 achieved a stable voltage range of 0.516–0.611V after three cycles. During the same period, MFC-2 achieved a stable voltage range of 0.723–0.814V after three cycles. The modified anode showed a higher OCV compared to the original anode, leading to the conclusion that it achieved the maximum OCV (OCV of MFC-2 significantly increased by 33 % (1.3 times) higher than that of MFC-1). The results suggest that both MFCs have been successfully commissioned and are now ready for actual wastewater treatment experiments. However, the high open circuit voltage (OCV) in MFC-2 indicates that there is excellent adhesion of electrogenic microorganisms and a significant accumulation of electrons on the surface of the modified carbon cloth (CC) due to the deposition of the nano-pumice. Furthermore, the incorporation of an anode catalyst nano-pumice in MFC-2 results in a significant reduction of the start-up time by an average of 47 % as compared to MFC-1. The use of nano-pumice as an anode catalyst increased the surface area and space available for electrogenic bacteria to attach to the anodic surface. This allowed for a greater number of bacteria to be accommodated on the anode surface, thereby promoting stronger interaction between the bacteria and the anode. As a result, a more stable biofilm capable of generating electricity was formed. The measured open circuit voltage (OCV) of MFC-2 was similar to that of other materials employed as anode catalysts, such as MnO_2/PPy/Carbon felt (451 mV) [52], rGO/MnO_2/Carbon felt (700 mV) [53], NiO/MnO_2/Carbon felt (652 mV) [54], NiO/CNT/-PANI/Carbon cloth (642 mV) [55], and NiO/PANI/Carbon felt (725 mV) [56].

Actual wastewater was introduced into the system by dilution at different COD concentrations and the OCV for each of these COD concentrations was also analyzed (Fig. 4). Different voltages were recorded in both types of MFCs at different COD concentrations. The maximum voltage generated in MFC-1 was 0.804 ± 0.02V at a COD concentration of 4000 mg/L. Similarly, the maximum voltage generated in MFC-2 was 1.126 ± 0.01V when the COD concentration was 12000 mg/L. As the COD concentration increased, the OCV decreased with increasing substrate loading. Possible explanations for this phenomenon include the influence of increased COD levels on microbial activity within the anode chamber, increased internal resistance of the anode chamber and increased charge transfer resistance. After analyzing the data, it was determined that the most effective COD concentration for further studies with varying external loads was 4000 mg/L for MFC-1 and 12000 mg/L for MFC-2. It was also found that MFC-1 achieved a stable OCV at different COD concentrations after a period of 5 days, while MFC-2 achieved the same stability within 3 days.

The MFC-1 system, with a COD concentration of 4000 mg/L and a reaction time of 5 days, and the MFC-2, with a COD concentration of 12000 mg/L and a reaction time of 3 days, were tested to determine their closed circuit voltage (CCV) production. This was done by varying the external resistance from 1000 to 25Ω. As shown in Fig. 5, the voltage produced by MFC-1 remained fairly constant as the external resistance was reduced from 1000 to 200Ω. There was a significant decrease in voltage when the external resistance changed from 200 to 25Ω. During the MFC-2 experiment, the voltage generated remained rather constant when the external resistance decreased from 1000 to 50Ω. However, there was a significant drop in voltage occurred when the external resistance was further reduced to 25Ω. The MFC-1 achieved a maximum closed circuit voltage of 0.765 ± 0.04V with a resistance of 200Ω, while the MFC-2 achieved a maximum closed circuit voltage of 1.114 ± 0.01V with a resistance of 50Ω. When a 200Ω external resistance was added to the MFC-1 electrical circuit, the removal of COD reached 65 ± 4 %. Similarly, in MFC-2, with a resistance of 50 Ω, the COD removal reached 93 ± 3 %. In all MFC systems, the values of these parameters were higher than in other systems. Additionally, the percentage of COD removal increased by ~4 % and 11 % in MFC-1 and MFC-2, respectively, compared to the open circuit mode (Fig. 5).

The polarization curve shows the variations in voltage and power density as a function of current density (Fig. 6). For MFC-1 the ideal resistance is 200Ω, while for MFC-2 it is 50Ω. From Fig. 5, it can be seen that in MFC-1, the current density peaked at 35±6A/m^3

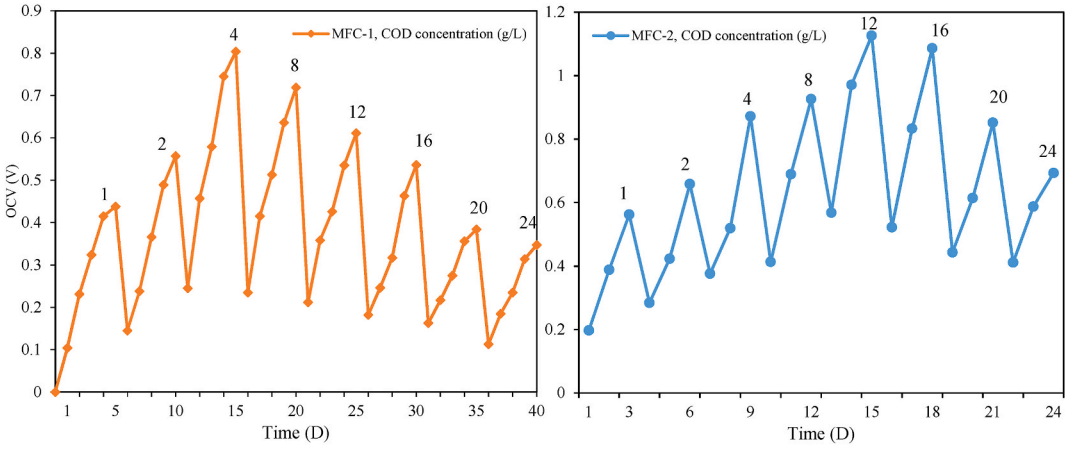

Fig. 4. Performance of MFC-1 and MFC-2 during open circuit voltage with different COD concentrations.

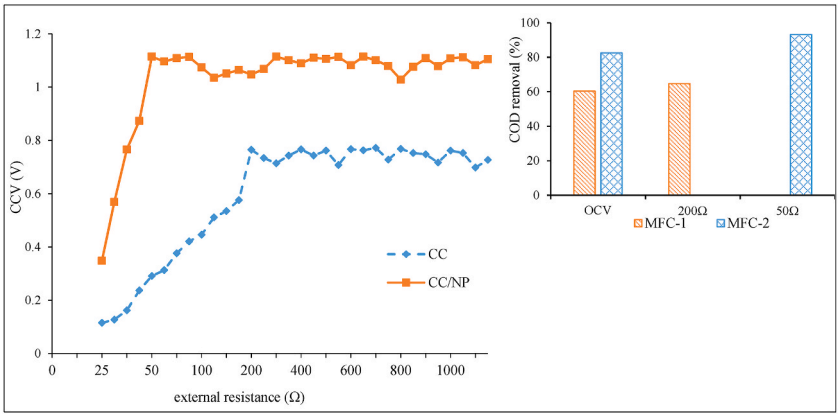

Fig. 5. Performance of MFC-1 and MFC-2 during close circuit voltage for different external load in the optimum COD concentration.

and the power density peaked at 18±4W/m^3 before declining. However, in MFC-2 the current density also reached a value of 55±5A/m^3, and the power density rose to 30±4W/m^3 before declining (Fig. 6). This increase was approximately 61 ± 3 % greater than that observed in MFC-1. The anode coated with nanoparticles (NP) significantly improved the maximum power density of the microbial fuel cell (MFC). This improvement was observed in the MFC with the NP-coated anode, indicating a significant increase in power density. The voltage in the polarization curve decreased as the current density increased, mainly due to variables such as membrane fouling and other losses encountered during MFC operation, including activation losses, ohmic losses and concentration losses. The superior performance of MFC-2 using nano-pumice as the anode catalyst compared to MFC-1 in this investigation can be attributed to the increased surface area of the anode. This increased surface area allows for improved conductivity for the generation and transfer of electrons. The increased surface area of the anode facilitates more efficient electron transfer, resulting in a reduction in the internal resistance of the system [23]. In addition, the increase in power density can be attributed to the addition of electrochemically active bacteria to the anode surface, which enhances electron transfer in the MFC system. The findings of the current investigation were consistent with prior studies. Y. Wang et al. (2020) reported a power density of 14W/m^3 [57], while J. Jiang et al. (2011) reported a power density of 11.8W/m^3 in a two-chambered microbial fuel cell [58]. Y. Zhang et al. (2011) reported a power density of 14W/m^3 [59]. In a study conducted by M. Behera in 2009, the power density of 11.04W/m^3 was found in a two-chambered microbial fuel cell [60].

Coulombic efficiency (CE) is a measure of the proportion or percentage of electrons that are successfully recovered as a current, in relation to the total number of electrons generated during the degradation of a substrate. Fig. 7 shows the CE variation with the current density for resistances of 200 Ω and 50 Ω for MFC-1 and MFC-2, respectively. The highest achievable CE was 47 ± 5 % and 78 ± 3 % in MFC-1 and MFC-2, respectively. The results showed that for both MFC-1 and MFC-2 systems, the CE showed an upward trend with increasing current density. However, this increase was 31 ± 2 % higher in MFC-2 than in MFC-1. The highest CE achieved in MFC-2 was more satisfactory, confirming the performance of the MFC in effectively utilizing a significant amount of organic matter for electricity production throughout the treatment. The CE of an MFC is influenced by various elements such as the biodegradability of the substrate, conductivity of the electrode materials, external resistance, operating conditions and microbial activity [61]. In this study, the increase in CE in MFC-2 to the enhanced surface area and conductivity of the redesigned electrode, which in turn reduces internal resistance. The highest CE achieved in MFC-2 was similar to that of MFCs treating food waste leachate (66 %) [62], MFCs

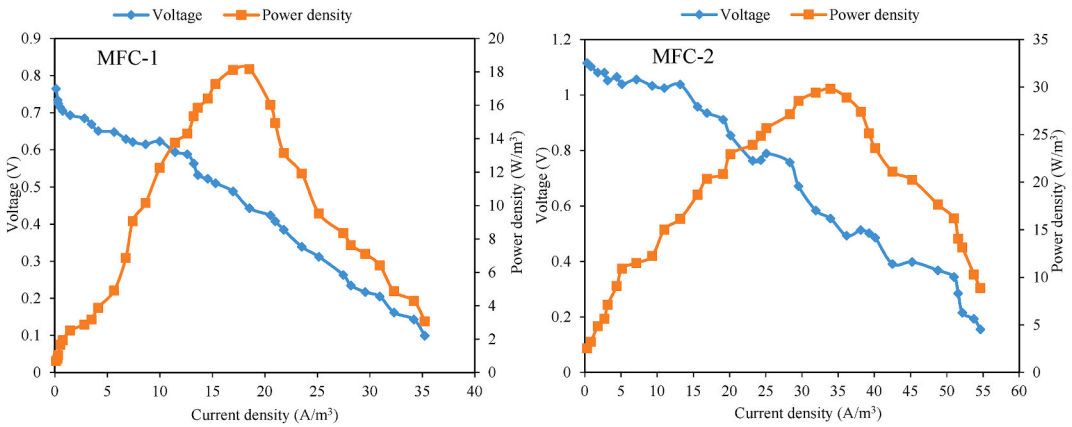

Fig. 6. Electricity generation performance of different anodes in the MFC (polarization curves).

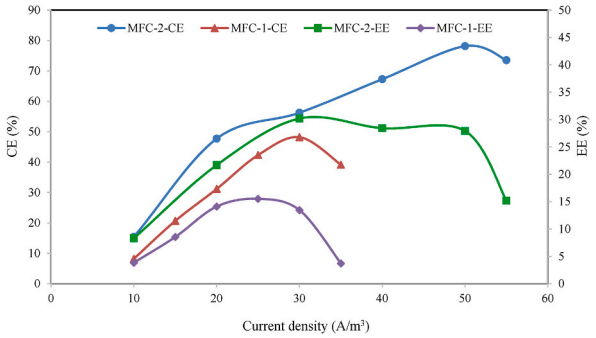

Fig. 7. Coulombic efficiency and energy efficiency as a function of current density.

treating synthetic wastewater (44.9 %) [56], and MFCs treating effluent drain from the vegetable oil sector (36.5 %) [63]. The EE of a MFC is determined by the ratio of the energy recovered to the energy content of the biodegradable substrates. The EE at the point of maximum CE was observed to be 13 ± 2 % in MFC-1 and 28 ± 1 % for MFC-2. This represents an increase of 14 ± 3 % in MFC-2 compared to MFC-1. The findings of the current investigation are superior to those of J. Choi and Y. Ahn (2015), who reported an EE of 13.8 % at the point of maximum CE [64].

3.3.1. Influence of OLR on the electricity generation

MFC-1 and MFC-2 were operated at various organic loading rates (OLRs) ranging from 0.34 to 8gCOD/L-d. MFC-1 was operated at an external resistance of 200Ω, whereas MFC-2 was operated at an external resistance of 50Ω. Fig. 8 shows the voltage, power density, and current density was measured as a function of OLR when a two-chamber MFC was used in batch mode to treat wastewater from an edible vegetable oil refinery. Fig. 8 clearly shows that in MFC-1, as the OLR increased from 0.34 to 1.34gCOD/L-d, the voltage generated increased from 0.273 to 0.783V, which is an increase of over 90 %. Similarly, in MFC-2, as the OLR increased from 0.34 to 4gCOD/L-d, the voltage generated increased from 0.563 to 1.117V, which is also an increase of over 90 %.

The reason for this is that higher OLRs can effectively provide more materials for electrogenic bacteria to use, thereby promoting chemical energy recovery. However, as the OLR increased from 1.34 to 8gCOD/L-d in MFC-1 and from 4 to 8gCOD/L-d in MFC-2, the power density, current density and voltage generated in both systems decreased. The rate of reduction was greater in MFC-1 than in MFC-2. This suggests that an extremely high OLR can lead to the accumulation of volatile fatty acids in the MFCs due to the reduced interaction time between microorganisms and substrate, as well as limitations in mass transfer. As a result, this can inhibit power generation in the MFC. In addition, increased OLR in the anode chamber can lead to a higher probability of membrane fouling, which can have a negative impact on voltage generation. Furthermore, the presence of higher OLR leads to an increase in the activity of methanogenic microorganisms. This increase has a negative effect on the power generation capacity of electrogenic bacteria [44]. Therefore, the MFC may reach its highest voltage output at a certain OLR. However, when the OLR exceeds this threshold, the voltage output decreases. The study found that the MFC-1 can handle a maximum load of 1.34gCOD/L-d of edible vegetable oil refinery effluent, while the MFC-2 can handle up to 4gCOD/L-d. Therefore, loading rates of 1.34gCOD/L-d and 4gCOD/L-d were chosen for MFC-1 and MFC-2, respectively, as these rates resulted in the highest power generation. When comparing the performance of the anode catalyst nano-pumice with the MFCs published in the literature (I. Gajda et al., 2020; R. Aryal et al., 2019; Y. Wang et al., 2020; X. Xing et al., 2020), it is evident that the former exhibits superior performance [57,65–67].

The coulombic efficiency (CE) in MFC-1 decreased with increasing OLR from 41 ± 2 % at 0.34gCOD/L-d to 9 ± 1 % at 8gCOD/L-d.

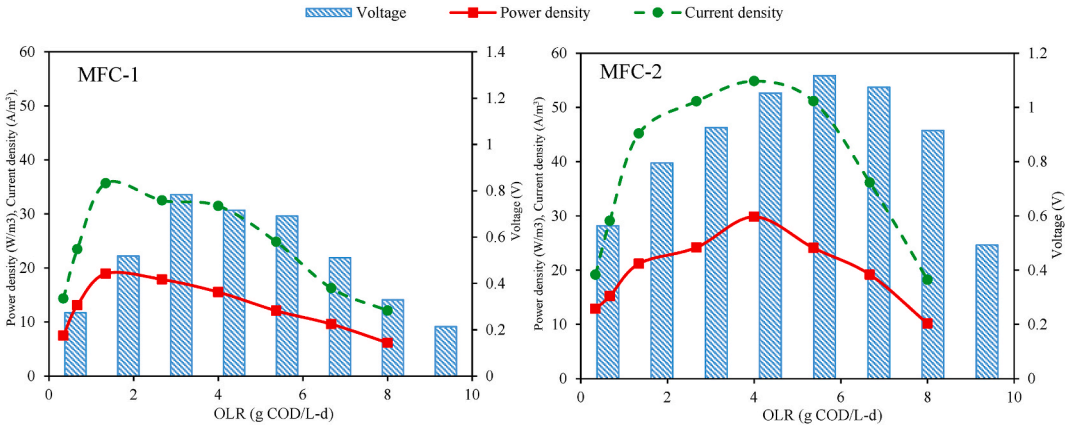

Fig. 8. MFC performance with different anodes in various organic loading rates (cell potential, power density and current density).

Similarly, the CE in MFC-2 decreased from 79 ± 5 % to 19 ± 2 % (Fig. 9). There was also a decrease in EE with increasing organic loading. The presence of a highly saturated anode surface can lead to the stimulation of side populations such as methanogens and heterotrophs. These populations can then compete with the electrogenic bacteria for substrates, ultimately reducing the activity of the electrogenic microorganisms. Electrogenic bacteria show superior dominance over other microbial communities at lower OLRs. Furthermore, at higher OLRs, current production is limited by a decrease in the rate of electron transfer from the supplied organic matter. At higher OLRs, a smaller proportion of the substrate is used to produce electricity [21]. Also, Energy efficiency (EE) decreased as OLRs increase (in MFC-1 from 18 ± 3 % at 0.34gCOD/L-d to 3 ± 0.7 % at 8gCOD/L-d and in MFC-2 from 32 ± 2 % at 0.34gCOD/L-d to 10 ± 1 % at 8gCOD/L-d). The highest CE was obtained in MFC-2, where the electrode catalyst was consisted of nanoparticles (NP). This configuration facilitated the utilization of a greater proportion of organic matter by electrogenic bacteria, which were able to adhere to the larger surface area of the anode provided by the NP. As a result, there was an efficient transfer of electrons and protons occurred between the bacteria and the electrode. The findings of this work were consistent with previous research conducted by X. M. Li et al. [68], K.B. Ghoreishi et al. [69], and M. Ghasemi et al. [70], where a CE of 63.4 %, 16 %, and 21 % was recorded, respectively.

3.3.2. COD removal

The measure of organic matter removal efficiency in MFCs is often represented in terms of COD removal. Fig. 10 shows the COD removal efficiency of the MFC during the process of power production and wastewater treatment at various OLRs. It was found that in MFC-1, the COD removal efficiency was 66 ± 3 % when the OLR increased from 0.34 to 1.34gCOD/L-d. However, in MFC-2, the COD removal efficiency was 94 ± 2 % when the OLR grew from 0.34 to 4gCOD/L-d. The further reduction in COD in MFC-2 can be attributed to the nano-pumice electrode catalyst, which provides a large surface area and many sites for bacterial adhesion, promoting the formation of a biofilm. This in turn enhances the bio-electrocatalytic oxidation of the organic substrate, resulting in improved COD removal. However, in MFC-1, when OLRs ranged from 1.34 to 8gCOD/L-d, and in MFC-2, when OLRs ranged from 4 to 8gCOD/L-d, this situation resulted in a decrease in COD removal efficiency to about 34 ± 2 % in MFC-1 and 68 ± 6 % in MFC-2. This can be attributed to the suppression of microbial activity due to the increased organic loading in the MFCs. The decrease in COD removal efficiency in MFC-2 was less significant compared to MFC-1, which can be attributed to the larger anode surface area in MFC-2. The results of this work was consistent with our prior findings that the production of power from MFCs had a significant correlation with the strength of wastewater, specifically the concentration of COD [45]. The findings of this study provide superior results compared to the studies conducted by S. Zou et al. (2018) [71], N. Yang et al. (2018) [72], and Y. Wu et al. (2017) [73], which showed COD removal efficiencies of 69 %, 89 %, and 64 % respectively.

3.3.3. Nutrients (NH_4^+-N and P) removal

Nutrient pollution is a common issue in numerous industrial wastewaters. The impact of OLR on the removal of nutrients (ammonia and phosphorus) from the incoming flow of the two-chamber MFC was investigated as shown in Fig. 10. Based on the data presented, it can be observed that in MFC-1, there was an increase in the removal of NH_4^+-N and P in the anode effluent as the OLR increased from 0.34 to 4gCOD/L-d. Similarly, in MFC-2, there was an increase in the removal of NH_4^+-N and P in the anode effluent as the OLR increased from 0.34 to 5.37gCOD/L-d. In MFC-1, the removal effectiveness of NH_4^+-N ranged from 16 ± 2 % to 57 ± 6 %, with a maximum of 57 ± 6 %. Similarly, the removal efficiency of P ranged from 12 ± 1 % to 48 ± 3 %, with a maximum of 48 ± 3 %. The removal efficiencies of NH_4^+-N and P in MFC-2 ranged from 42 ± 2 % to 85 ± 4 %, with a maximum of 85 ± 4 % for NH_4^+-N and from 27 ± 3 % to 76 ± 5 %, with a maximum of 76 ± 5 % for P. In MFC-1, when the OLR was increased to 8gCOD/L-d, the values decreased to 34 ± 2 % and 29 ± 1 %, respectively. In MFC-2, when the OLR was increased to 8gCOD/L-d, the values decreased to 45 ± 3 % and 41 ± 4 %, respectively. Bacterial growth facilitated the removal of NH_4^+-N and P in the anode chamber via microbial action. As depicted in Fig. 10, MFC-2, equipped with nano-pumice catalyst, showed the maximum efficiency in removing NH_4^+-N and P. The use of nano-pumice as an anode catalyst resulted in the formation of a biofilm due to the increased surface area available for bacterial adhesion. In addition, some of the NH_4^+-N losses occurred through movement of NH_4^+ ions across the Proton Exchange Membrane (PEM) from the anode to the cathode. This could potentially serve as a method for eliminating NH_4^+-N in the MFCs [74].

The use of nitrogen (N) and phosphorus (P) for biomass growth is determined by the organic to nutrient ratio (COD:N:P) in the

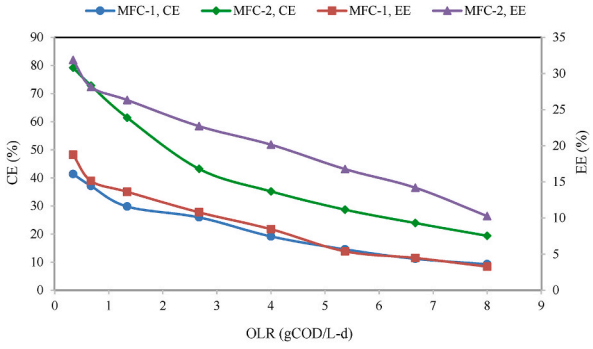

Fig. 9. MFC performance with different anodes in various organic loading rates (coulombic efficiency and energy efficiency).

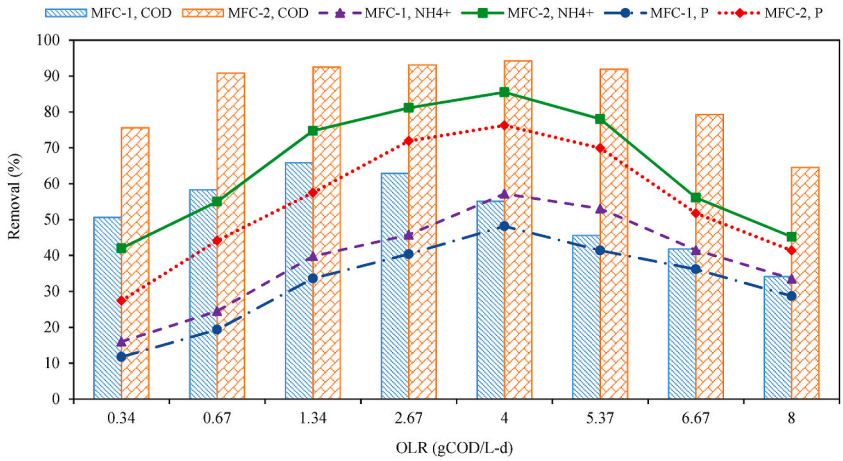

Fig. 10. COD and nutrients removal efficiency in MFC-1 and MFC-2 as a function of OLR.

context of treating biodegradable organic waste in wastewater treatment. In this situation, an increase in OLR could lead to an increase in the biological nutrients uptake. In addition, studies have indicated that the nutritional requirements for microbial growth in high-strength organic wastewater (with a COD greater than 4000 mg/L) are greater than those in low-strength organic wastewater [24]. The findings of this study indicate that the implementation of a two-chamber MFC can effectively reduce the levels of nitrogen and phosphorus in wastewater treatment plants, which is in line with previous studies [17,19].

3.3.4. Sulfate (SO_4^{2-}) removal

Sulfate is a prevalent pollutant present in wastewater from edible vegetable oil refineries. Elevated levels of sulfate have adverse effects on both the ecosystem and human health. The concentration of SO_4^{2-} in the effluent from the anode of the MFC was measured at various OLRs during the electricity production process and the results are depicted in Fig. 11. The removal efficiencies of SO_4^{2-} improved as the OLR increased from 0.34 to 4gCOD/L-d, reaching values of up to 45 ± 3 % in MFC-1 and 68 ± 6 % in MFC-2. The MFC-2, equipped with a catalyst of nano-pumice, exhibited the most effective removal of SO_4^{2-}. In MFC-1, when the OLR was increased to 8gCOD/L-d, the values decreased to 25 ± 2 %. However, in MFC-2, the values plummeted to 38 ± 4 %. Thus, it is evident that an increase in OLR could lead to a decrease in the removal efficiency.

Certain microorganisms, such as sulfate-reducing bacteria (SRB), can utilize the sulfate contained in wastewater the sludge as the ultimate electron acceptor. The sulfate is then converted to sulfide. Sulfide exhibits electrochemical activity at the anode and undergoes oxidation to form elemental sulfur. This sulfur is then deposited on the electrode surface, resulting in power generation [61]. This particular type of MFC exhibits higher current density compared to other types and does not require the use of heterogeneous mediators, as redox sulfate or sulfide serve as mediators. The findings align with the research conducted by J.M. Morris et al., on the impact of nitrate and sulfate on electricity generation in MFC [75]. Additionally, G. Hernandez-Flores et al., explored the use of fusion

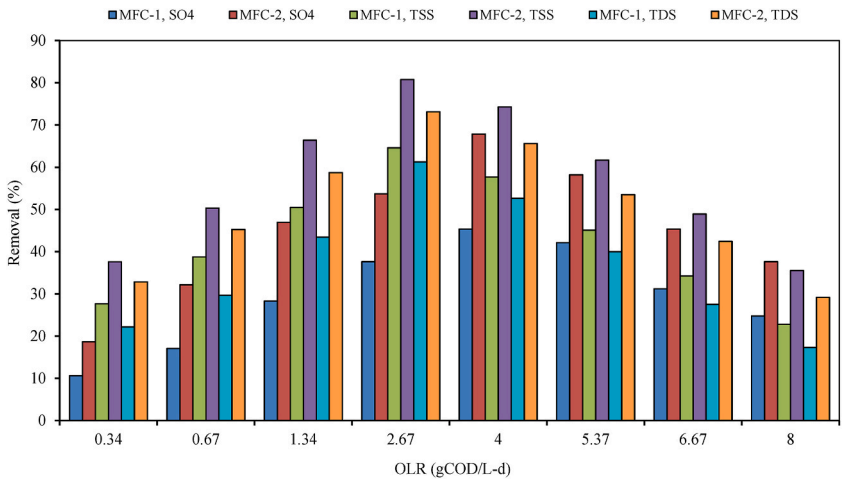

Fig. 11. Sulfate, TSS and TDS removal efficiency in MFC-1 and MFC-2 during in various organic loading rates of the edible vegetable oil refinery wastewater.

of alternating membranes instead of Nafion in MFC [76], and the production of energy from leachate using anion exchange membrane MFC [77].

3.3.5. TSS and TDS removal

The wastewater from the edible vegetable oil refinery was found to have elevated levels of solid concentrations. The treatment efficiencies of both MFC-1 and MFC-2 were evaluated based on the removal of TSS and TDS, using an organic load ranging from 0.34 to 8gCOD/L-d. Experimental data collected during the procedure showed a significant decrease in TSS and TDS. Fig. 11 shows that MFC-1 achieved a maximum reduction of 65 ± 3 % in TSS and 61 ± 1 % in TDS with an organic loading of 2.67gCOD/L-d. On the other hand, MFC-2 achieved a higher reduction of 81 ± 2 % in TSS and 73 ± 1 % in TDS at the same organic loading. The removal efficiencies of TSS and TDS were higher in MFC-2 compared to MFC-1 due to the larger electrode surface area, which allowed for more attachment sites for electrogenic bacteria in MFC-2. When the organic loading exceeded 2.67gCOD/L-d, the removal of TSS and TDS declined in both MFC-1 and MFC-2. However, the decrease was more pronounced in MFC-1. The results indicate that the removal efficiency of TSS and TDS is influenced by the organic loading. TSS removal is achieved through the process of biodegradation in the MFC. At higher OLRs, this process is accompanied by the deposition of fermentative products and the performance of the anode chamber as a suspended anaerobic growth reactor. Additionally, complex colloidal and organic materials are degraded through a biological catalysis process. The reduction of TDS was attributed to the anaerobic process occurring in the cell metabolism of electrogenic bacteria and the existence of electroactive biofilms in the MFCs, which promoted the establishment of bioelectrogenic conditions. Moreover, the significant reduction in dissolved solids is probably due to the greater presence of easily degradable substances in the undiluted wastewater, resulting in increased microbial competition. The study conducted by T. Aswin et al. (2017) [78] found that the removal effectiveness of TSS and TDS in leather effluent was 66 % and 50 % respectively, while in dairy effluent it was 73 % and 58 % respectively. These values are lower than the findings of the current study. T. Karuppiah et al. found a maximum reduction of 68 % in TSS [79], whereas A.J.O. Al-saned et al. (2020) claimed the removal of 79.3 % of TSS and 62.5 % of TDS [80].

4. Conclusions

This work emphasizes the use of pumice obtained from pumice mine waste as a low-cost anode catalyst in MFCs, while also recognizing its local mineral properties. Nanoscale pumice was prepared and used. Nano-pumice increases the surface area of the anode, allowing for better adsorption of microorganisms to create a biofilm. It also improves bio-catalytic activity and facilitates efficient electron transfer, ultimately increasing the efficiency of anodes in MFCs. The use of this nano-pumice-modified anode can lead to a significant increase in the OCV (33 %) of the MFC, resulting in a much higher power production. In addition, it can effectively minimize the pollution levels during the treatment process. The use of nano-pumice as an anode catalyst in the MFC treating edible vegetable oil refinery wastewater resulted in the highest power density (30±4W/m^3), CE (79 ± 5 %), EE (32 ± 2 %), and COD removal (94 ± 2 %). T This indicates that the use of nano-pumice, a local mineral and low-cost catalyst, not only enhanced the anode performance in electricity generation and CE, but also significantly reduced the start-up time. Therefore, due to its simple design, reduced cost and increased power generation capacity, it has the potential to be used in future large-scale BES with improved efficiency and optimal cost-effectiveness.

CRediT authorship contribution statement

Fatemeh Eslami: Investigation, Funding acquisition, Conceptualization. **Kamyar Yaghmaeian:** Supervision, Project administration, Conceptualization. **Reza Shokoohi:** Visualization, Data curation. **Roohallah Sajjadipoya:** Software, Resources, Investigation. **Alireza Rahmani:** Writing – original draft, Methodology. **Hedieh Askarpur:** Investigation, Formal analysis. **Abbas Norouzian Baghani:** Validation, Formal analysis. **Hossein Jafari Mansoorian:** Writing – review & editing, Writing – original draft, Supervision, Methodology, Investigation. **Farshid jaberi Ansari:** Investigation.

Data availability statement

The authors are unable or have chosen not to specify which data has been used.

Declaration of competing interest

The authors declare that they have no known competing financial interests or personal relationships that could have appeared to influence the work reported in this paper.

Acknowledgement

The authors express their gratitude for the financial support provided by the Jiroft University of Medical Sciences, located in Jiroft, Iran. The funding was supplied under the Ethics Code: IR.JMU.REC.1399.013.

References

[1] E.A. Sharghi, P. Ghasemian, L. Davarpanah, G. Faridizad, Investigation of a membrane bioreactor's performances in treating sunflower oil refinery wastewater containing high oleic acid at different SRTs, Bioproc. Biosyst. Eng. 46 (11) (2023) 1613–1625.
[2] MCLSW. Ministry of Cooperatives Labour and Social Welfare, Iranian Vegetable Oil Industry Association, 2024. https://www.ivoia.com.
[3] E. Abdollahzadeh Sharghi, A. Shourgashti, B. Bonakdarpour, Considering a membrane bioreactor for the treatment of vegetable oil refinery wastewaters at industrially relevant organic loading rates, Bioproc. Biosyst. Eng. 43 (6) (2020) 981–995.
[4] Y. Bai, Y. Zhai, C. Ji, T. Zhang, W. Chen, X. Shen, et al., Environmental sustainability challenges of China's edible vegetable oil industry: from farm to factory, Resour. Conserv. Recycl. 170 (2021) 105606.
[5] O.F. Saeed, K.W. Hameed, A.H. Abbar, Treatment of vegetable oil refinery wastewater by sequential electrocoagulation-electrooxidation process, J. Environ. Manag. 342 (2023) 118362.
[6] T. Ahmad, T. Belwal, L. Li, S. Ramola, R.M. Aadil, Abdullah, et al., Utilization of wastewater from edible oil industry, turning waste into valuable products: a review, Trends Food Sci. Technol. 99 (2020) 21–33.
[7] M.M. Emamshoushtari, S. Helchi, F. Pajoum Shariati, M. Lotfi, A. Hemmati, An investigation into the efficiency of microalgal dynamic membrane photobioreactor in nickel removal from synthesized vegetable oil industry wastewater: a water energy nexus case study, Energy Nexus 7 (2022) 100116.
[8] Z. Šereš, N. Maravić, A. Takači, I. Nikolić, D. Šoronja-Simović, A. Jokić, et al., Treatment of vegetable oil refinery wastewater using alumina ceramic membrane: optimization using response surface methodology, J. Clean. Prod. 112 (2016) 3132–3137.
[9] P. Dhanke, S. Wagh, Treatment of vegetable oil refinery wastewater with biodegradability index improvement, Mater. Today Proc. 27 (2020) 181–187.
[10] I. Khouni, G. Louhichi, A. Ghrabi, P. Moulin, Efficiency of a coagulation/flocculation–membrane filtration hybrid process for the treatment of vegetable oil refinery wastewater for safe reuse and recovery, Process Saf. Environ. Protect. 135 (2020) 323–341.
[11] K. Rajkumar, M. Muthukumar, R. Sivakumar, Novel approach for the treatment and recycle of wastewater from soya edible oil refinery industry—an economic perspective, Resour. Conserv. Recycl. 54 (10) (2010) 752–758.
[12] O. Hartal, A. Madinzi, S. Khattabi Rifi, C. Haddaji, T. Agustiono Kurniawan, A. Anouzla, et al., Optimization of coagulation-flocculation process for wastewater treatment from vegetable oil refineries using chitosan as a natural flocculant, Environ. Nanotechnol. Monit. Manag. 22 (2024) 100957.
[13] C. Haddaji, M. Chatoui, S. Khattabi Rifi, Z. Ettaloui, K. Digua, A. Pala, et al., Performance of simultaneous carbon, nitrogen, and phosphorus removal from vegetable oil refining wastewater in an aerobic-anoxic sequencing batch reactor (OA-SBR) system by alternating the cycle times, Environ. Nanotechnol. Monit. Manag. 20 (2023) 100827.
[14] A.M.A. Pintor, A.G. Martins, R.S. Souza, V.J.P. Vilar, C.M.S. Botelho, R.A.R. Boaventura, Treatment of vegetable oil refinery wastewater by sorption of oil and grease onto regranulated cork – a study in batch and continuous mode, Chem Eng J 268 (2015) 92–101.
[15] S.V. Ramanaiah, K. Chandrasekhar, C.M. Cordas, I. Potoroko, Bioelectrochemical systems (BESs) for agro-food waste and wastewater treatment, and sustainable bioenergy-A review, Environ. Pollut. 325 (2023) 121432.
[16] S. Kondaveeti, D. Govindarajan, G. Mohanakrishna, D. Thatikayala, I.M. Abu-Reesh, B. Min, et al., Sustainable bioelectrochemical systems for bioenergy generation via waste treatment from petroleum industries, Fuel 331 (2023) 125632.
[17] P.D. Kolubah, H.O. Mohamed, M.N. Hedhili, M. Ben Hassine, R. Díaz-Rúa, D.I. Drautz-Moses, et al., Sustainable energy production from domestic wastewater via bioelectrochemical reactors using MXene efficient electrodes decorated with transition metal nanoparticles, J. Environ. Chem. Eng. 12 (5) (2024) 113793.
[18] P. Mullai, S. Vishali, S.M. Sambavi, K. Dharmalingam, M.K. Yogeswari, V.C. Vadivel Raja, et al., Energy generation from bioelectrochemical techniques: concepts, reactor configurations and modeling approaches, Chemosphere 342 (2023) 139950.
[19] T. Ren, Y. Liu, C. Shi, C. Li, Bimetal-organic framework-derived porous CoFe2O4 nanoparticles as biocompatible anode electrocatalysts for improving the power generation of microbial fuel cells, J. Colloid Interface Sci. 643 (2023) 428–436.
[20] D. Jiang, H. Chen, H. Xie, H. Liu, M. Zeng, K. Xie, MnO2@MXene/Carbon cloth as an anode for microbial fuel cells, ChemistrySelect 7 (2022).
[21] H. Xu, Y. Du, Y. Chen, Q. Wen, C. Lin, J. Zheng, et al., Electricity generation in simulated benthic microbial fuel cell with conductive polyaniline-polypyrole composite hydrogel anode, Renew. Energy 183 (2022) 242–250.
[22] Y. Wang, Z. Wang, X. Kong, Y. Song, Y. Tian, J. Lin, Capacitive and biocompatibility composite anode material for enhanced renewable energy conversion for MFCs, Fuel 376 (2024) 132736.
[23] J.S. Santos, M. Tarek, M.S. Sikora, S. Praserthdam, P. Praserthdam, Anodized TiO2 nanotubes arrays as microbial fuel cell (MFC) electrodes for wastewater treatment: an overview, J. Power Sources 564 (2023) 232872.
[24] K. Zhu, S. Wang, H. Liu, S. Liu, J. Zhang, J. Yuan, et al., Heteroatom-doped porous carbon nanoparticle-decorated carbon cloth (HPCN/CC) as efficient anode electrode for microbial fuel cells (MFCs), J. Clean. Prod. 336 (2022) 130374.
[25] X. Wu, X. Li, Z. Shi, X. Wang, Z. Wang, W. Lin, et al., Doping molybdenum oxides with different non-metal atoms to promote bioelectrocatalysis in microbial fuel cells, J. Colloid Interface Sci. 645 (2023) 371–379.
[26] Y. Wang, X. Cheng, K. Liu, X. Dai, J. Qi, Z. Ma, et al., 3D hierarchical Co(8)FeS(8)-FeCo(2)O(4)/N-CNTs@CF with an enhanced microorganisms-anode interface for improving microbial, Fuel Cell Performance 14 (31) (2022) 35809–35821.
[27] W. Guo, X. Li, L. Cui, Y. Li, H. Zhang, T. Ni, Promoting the anode performance of microbial fuel cells with nano-molybdenum disulfide/carbon nanotubes composite catalyst, Bioproc. Biosyst. Eng. 45 (1) (2022) 159–170.
[28] D. Jiang, C. Zhu, Y. He, C. Xing, K. Xie, Y. Xu, Polyaniline-MXene-coated carbon cloth as an anode for microbial fuel cells, J. Solid State Electrochem. 26 (2022).
[29] J. Yang, S. Cheng, S. Zhang, W. Han, B. Jin, Modifying Ti3C2 MXene with NH4+ as an excellent anode material for improving the performance of microbial fuel cells, Chemosphere 288 (2022) 132502.
[30] Geetanjali Rinki, P.P. Kundu, Nickel-Cobalt oxides coated on polypyrrole nanotubes as bifunctional electrode catalyst for enhancing the performance of the microbial fuel cells, Mater. Sci. Eng., B 297 (2023) 116735.
[31] W. Guo, Y. Chen, L. Cui, N. Xu, M. Wang, Y. Sun, et al., Nano-hydroxyapatite/carbon nanotube: an excellent anode modifying material for improving the power output and diclofenac sodium removal of microbial fuel cells, Bioelectrochemistry 154 (2023) 108523.
[32] Y. Liu, Y. Sun, M. Zhang, S. Guo, Z. Su, T. Ren, et al., Carbon nanotubes encapsulating FeS2 micropolyhedrons as an anode electrocatalyst for improving the power generation of microbial fuel cells, J. Colloid Interface Sci. 629 (2023) 970–979.
[33] T. Cai, L. Meng, G. Chen, Y. Xi, N. Jiang, J. Song, et al., Application of advanced anodes in microbial fuel cells for power generation: a review, Chemosphere 248 (2020) 125985.
[34] R.S. Chouhan, S. Gandhi, S.K. Verma, I. Jerman, S. Baker, M. Štrok, Recent advancements in the development of Two-Dimensional nanostructured based anode materials for stable power density in microbial fuel cells, Renew. Sustain. Energy Rev. 188 (2023) 113813.
[35] M.N. Ardakani, G. Badalians Gholikandi, Microbial fuel cells (MFCs) in integration with anaerobic treatment processes (AnTPs) and membrane bioreactors (MBRs) for simultaneous efficient wastewater/sludge treatment and energy recovery -A state-of-the-art review, Biomass Bioenergy 141 (2020) 105726.
[36] G. Asgari, A. Rafizadeh, M. Ghasemi, Carbon modified pumice as a new adsorbent for the rapid removal of fluoride ions from aqueous phase, Avicenna J Environ Health Eng 5 (1) (2018) 56–66.
[37] A. Khataee, P. Gholami, B. Kayan, D. Kalderis, L. Dinpazhoh, S. Akay, Synthesis of ZrO(2) nanoparticles on pumice and tuff for sonocatalytic degradation of rifampin, Ultrason. Sonochem. 48 (2018) 349–361.
[38] L. Díaz, D. Escalante, K.E. Rodríguez, Y. Kuzmina, L.A. González, Response surface methodology for continuous biodiesel production from Jatropha curcas oil using Li/pumice as catalyst in a packed-bed reactor assisted with diethyl ether as cosolvent, Chem. Eng. Process 179 (2022) 109065.
[39] J. Arun, P. SundarRajan, K. Grace Pavithra, P. Priyadharsini, S. Shyam, R. Goutham, et al., New insights into microbial electrolysis cells (MEC) and microbial fuel cells (MFC) for simultaneous wastewater treatment and green fuel (hydrogen) generation, Fuel 355 (2024) 129530.
[40] A. Janicek, N. Gao, Y. Fan, H. Liu, High performance activated carbon/carbon cloth cathodes for microbial fuel cells, Fuel Cell. 15 (2015).

[41] D. Li, Y. Qu, J. Liu, W. He, H. Wang, Y. Feng, Using ammonium bicarbonate as pore former in activated carbon catalyst layer to enhance performance of air cathode microbial fuel cell, J. Power Sources 272 (2014) 909–914.
[42] P. Zhang, J. Liu, Y. Qu, J. Zhang, Y. Zhong, Y. Feng, Enhanced performance of microbial fuel cell with a bacteria/multi-walled carbon nanotube hybrid biofilm, J. Power Sources 361 (2017) 318–325.
[43] A. American Public Health, A.D. Eaton, A. American Water Works, and F. Water Environment, Standard Methods for the Examination of Water and Wastewater, 2005, 21st ed.,APHA-AWWA-WEF.Washington, D.C.
[44] H.J. Mansoorian, A. Mahvi, R. Nabizadeh, M. Alimohammadi, S. Nazmara, K. Yaghmaeian, Evaluating the performance of coupled MFC-MEC with graphite felt/MWCNTs polyscale electrode in landfill leachate treatment, and bioelectricity and biogas production, J. environ. health sci. eng. 18 (2) (2020) 1067–1082.
[45] K. Yaghmaeian, A. Rajabizadeh, F. Jaberi Ansari, S. Puig, R. Sajjadipoya, A.N. Baghani, et al., Treatment of vegetable oil industry wastewater and bioelectricity generation using microbial fuel cell via modification and surface area expansion of electrodes, J. Appl. Chem. Biotechnol. 98 (4) (2023) 978–989.
[46] Y. Liu, L. Ren, Z. Zhang, X. Qi, H. Li, J. Zhong, 3D binder-free MoSe2 nanosheets/carbon cloth electrodes for efficient and stable hydrogen evolution prepared by simple electrophoresis deposition strategy, Sci. Rep. 6 (1) (2016) 22516.
[47] W.-H. Cho, I.C. Cheng, J.-Z. Chen, Performance comparison of reduced graphene oxide (rGO)-polyaniline (PANI) supercapacitors with LiCl, Li2SO4, and H2SO4 electrolytes, J. Electrochem. Soc. 170 (2023).
[48] S. Sorayyaei, F. Raji, A. Rahbar-Kelishami, S.N. Ashrafizadeh, Combination of electrocoagulation and adsorption processes to remove methyl orange from aqueous solution, Environ.l Tech. Innov. 24 (2021) 102018.
[49] F. Eslami, R.N. Nodehi, S. Nasseri, M. Salari, A.H. Mahvi, F.D. Ardejani, Optimization of chromium (VI) adsorption by novel nano-pumice modified by cationic surfactant from aqueous media using the response surface method: isotherm and kinetic studies, Desalination Water Treat. 177 (2020) 139–151.
[50] P. de Rozari, D.S. Krisnayanti, Refli, K.V. Yordanis, M.R.R. Atie, The use of pumice amended with sand media for domestic wastewater treatment in vertical flow constructed wetlands planted with lemongrass (Cymbopogon citratus), Heliyon 7 (7) (2021) e07423.
[51] I.M. Dagwa, K.K. Adama, Property evaluation of pumice particulate-reinforcement in recycled beverage cans for Al-MMCs manufacture, J. King Saud Univ. Sci. 30 (1) (2018) 61–67.
[52] W. Chen, Z. Liu, G. Su, Y. Fu, X. Zai, C. Zhou, et al., Composite-modified anode by MnO2/polypyrrole in marine benthic microbial fuel cells and its electrochemical performance, Int. J. Energy Res. 41 (6) (2017) 845–853.
[53] C. Zhang, P. Liang, X. Yang, Y. Jiang, Y. Bian, C. Chen, et al., Binder-free graphene and manganese oxide coated carbon felt anode for high-performance microbial fuel cell, Biosens. Bioelectron. 81 (2016) 32–38.
[54] D. Zhong, Y. Liu, X. Liao, N. Zhong, Y. Xu, Facile preparation of binder-free NiO/MnO2-carbon felt anode to enhance electricity generation and dye wastewater degradation performances of microbial fuel cell, Int. J. Hydrogen Energy 43 (51) (2018) 23014–23026.
[55] F. Nourbakhsh, M. Mohsennia, M. Pazouki, Nickel oxide/carbon nanotube/polyaniline nanocomposite as bifunctional anode catalyst for high-performance Shewanella-based dual-chamber microbial fuel cell, Bioproc. Biosyst. Eng. 40 (2017) 1669–1677.
[56] D. Zhong, X. Liao, Y. Liu, N. Zhong, Y. Xu, Enhanced electricity generation performance and dye wastewater degradation of microbial fuel cell by using a petaline NiO@ polyaniline-carbon felt anode, Bioresour. Technol. 258 (2018) 125–134.
[57] Y. Wang, Q. Wen, Y. Chen, W. Li, Conductive polypyrrole-carboxymethyl cellulose-titanium nitride/carbon brush hydrogels as bioanodes for enhanced energy output in microbial fuel cells, Energy 204 (2020) 117942.
[58] J. Jiang, Q. Zhao, L. Wei, K. Wang, D.-J. Lee, Degradation and characteristic changes of organic matter in sewage sludge using microbial fuel cell with ultrasound pretreatment, Bioresour. Technol. 102 (1) (2011) 272–277.
[59] Y. Zhang, L.G. Olias, P. Kongjan, I. Angelidaki, Submersible microbial fuel cell for electricity production from sewage sludge, Water Sci. Technol. 64 (1) (2011) 50–55.
[60] M. Behera, M.á. Ghangrekar, Performance of microbial fuel cell in response to change in sludge loading rate at different anodic feed pH, Bioresour. Technol. 100 (21) (2009) 5114–5121.
[61] H.J. Mansoorian, A.H. Mahvi, A.J. Jafari, N. Khanjani, Evaluation of dairy industry wastewater treatment and simultaneous bioelectricity generation in a catalyst-less and mediator-less membrane microbial fuel cell, J. Saudi Chem. Soc. 20 (1) (2016) 88–100.
[62] S.S. Rikame, A.A. Mungray, A.K. Mungray, Electricity generation from acidogenic food waste leachate using dual chamber mediator less microbial fuel cell, Int. Biodeterior. Biodegrad. 75 (2012) 131–137.
[63] S. Firdous, W. Jin, N. Shahid, Z. Bhatti, A. Iqbal, U. Abbasi, et al., The performance of microbial fuel cells treating vegetable oil industrial wastewater, Environ.l Tech. Innov. 10 (2018) 143–151.
[64] J. Choi, Y. Ahn, Enhanced bioelectricity harvesting in microbial fuel cells treating food waste leachate produced from biohydrogen fermentation, Bioresour. Technol. 183 (2015) 53–60.
[65] R. Aryal, D. Beltran, J. Liu, Effects of Ni nanoparticles, MWCNT, and MWCNT/Ni on the power production and the wastewater treatment of a microbial fuel cell, Int. J. Green Energy 16 (15) (2019) 1391–1399.
[66] I. Gajda, J. Greenman, I. Ieropoulos, Microbial Fuel Cell stack performance enhancement through carbon veil anode modification with activated carbon powder, Appl. Energy 262 (2020) 114475.
[67] X. Xing, Z. Liu, W. Chen, X. Lou, Y. Li, Q. Liao, Self-nitrogen-doped carbon nanosheets modification of anodes for improving microbial fuel cells' performance, Catalysts 10 (4) (2020) 381.
[68] X.M. Li, K.Y. Cheng, J.W.C. Wong, Bioelectricity production from food waste leachate using microbial fuel cells: effect of NaCl and pH, Bioresour. Technol. 149 (2013) 452–458.
[69] K.B. Ghoreishi, M. Ghasemi, M. Rahimnejad, M.A. Yarmo, W.R.W. Daud, N. Asim, et al., Development and application of vanadium oxide/polyaniline composite as a novel cathode catalyst in microbial fuel cell, Int. J. Energy Res. 38 (1) (2014) 70–77.
[70] M. Ghasemi, W.R.W. Daud, S.H. Hassan, T. Jafary, M. Rahimnejad, A. Ahmad, et al., Carbon nanotube/polypyrrole nanocomposite as a novel cathode catalyst and proper alternative for Pt in microbial fuel cell, Int. J. Hydrogen Energy 41 (8) (2016) 4872–4878.
[71] S. Zou, L. Guan, D.P. Taylor, D. Kuhn, Z. He, Nitrogen removal from water of recirculating aquaculture system by a microbial fuel cell, Aquaculture 497 (2018) 74–81.
[72] N. Yang, G. Zhan, D. Li, X. He, Y. Zhang, Q. Jiang, et al., Performance and microbial community of a novel non-aeration-based up-flow bioelectrochemical filter (UBEF) treating real domestic wastewater, Chem Eng J 348 (2018) 271–280.
[73] Y. Wu, Q. Yang, Q. Zeng, H.H. Ngo, W. Guo, H. Zhang, Enhanced low C/N nitrogen removal in an innovative microbial fuel cell (MFC) with electroconductivity aerated membrane (EAM) as biocathode, Chem Eng J 316 (2017) 315–322.
[74] H.J. Mansoorian, A.H. Mahvi, A.J. Jafari, M.M. Amin, A. Rajabizadeh, N. Khanjani, Bioelectricity generation using two chamber microbial fuel cell treating wastewater from food processing, Enzym. Microb. Technol. 52 (6–7) (2013) 352–357.
[75] J.M. Morris, P.H. Fallgren, S. Jin, Enhanced denitrification through microbial and steel fuel-cell generated electron transport, Chem Eng J 153 (1) (2009) 37–42.
[76] G. Hernández-Flores, H.M. Poggi-Varaldo, O. Solorza-Feria, Comparison of alternative membranes to replace high cost Nafion ones in microbial fuel cells, Int. J. Hydrogen Energy 41 (48) (2016) 23354–23362.
[77] G. Hernández-Flores, H.M. Poggi-Varaldo, T. Romero-Castañón, O. Solorza-Feria, N. Rinderknecht-Seijas, Harvesting energy from leachates in microbial fuel cells using an anion exchange membrane, Int. J. Hydrogen Energy 42 (51) (2017) 30374–30382.
[78] T. Aswin, S. Begum, M. Sikkandar, Optimization of microbial fuel cell for treating industrial wastewater and simultaneous power generation, Int. J. Chem. Sci. 15 (2017).
[79] T. Karuppiah, A. Pugazhendi, S. Subramanian, M.T. Jamal, R.B. Jeyakumar, Deriving electricity from dye processing wastewater using single chamber microbial fuel cell with carbon brush anode and platinum nano coated air cathode 8 (10) (2018) 437.
[80] A.J.O. Al-saned, B.A. Kitafa, A.S. Badday, Microbial fuel cells (MFC) in the treatment of dairy wastewater, IOP Conf. Ser. Mater. Sci. Eng. 1067 (1) (2021) 012073.